

Intrinsic mechanism for the poor luminescence properties of quantum-box systems

H. Benisty

Laboratoire Central de Recherches, Domaine de Corbeville, Thomson-CSF, F-91404 Orsay CEDEX, France

C. M. Sotomayor-Torrès

*Nanoelectronics Research Centre, Department of Electronics and Electrical Engineering,
The University of Glasgow, G12 8QQ Glasgow, United Kingdom*

C. Weisbuch

Laboratoire Central de Recherches, Domaine de Corbeville, Thomson-CSF, F-91404 Orsay CEDEX, France

(Received 20 May 1991; revised manuscript received 3 September 1991)

The poor radiative efficiency in quantum-box luminescence is tentatively explained as an intrinsic effect rather than the usually invoked effect of etch damages. From the recently calculated decreased relaxation rate in zero-dimensional (0D) systems under 100–200-nm lateral quantization, we propose that electrons captured from the barriers in the upper levels of quantum boxes are retained in their cascade to the fundamental states for more than nanoseconds. Due to the mutual orthogonality of quantum states in a box, no luminescence, or much less than in 2D or 3D, can be obtained from these stored electrons with reasonable assumptions for the hole population. Magnetic-confinement experiments in quantum-well lasers support our conclusion. A realistic model at low temperature describes more quantitatively the observed strong decay of the radiative efficiency in quantum boxes and pseudowires with decreased lateral dimensions.

There is growing, universal evidence that one-dimensional (1D) and 0D nanostructures lead to diminished luminescence quality when compared to 2D or 3D heterostructures.^{1–4} Although some recovery of the optical properties occurs upon regrowth over etched structures^{5–7} and encouraging quantum-wire lasers have been fabricated,^{8,9} the luminescence properties never reach any of the improvement predicted from the concentration of the spectral oscillator strength. In this paper, we point out that these disappointing results, instead of being due to the often-invoked *extrinsic fabrication defects*, which might eventually be cured, are due, rather, to unescapable *intrinsic effects*, mainly orthogonality of electron and hole states combined with slowed-down relaxation in 1D and 0D.

All the descriptions of quantum-well, -wire, and -box lasers^{10–12} rely on the relaxation of carriers to the ground state, although it was known that light-hole-to-heavy-hole relaxation was affected by increased lateral confinement.¹³ More recently, slowed relaxation was also invoked to explain high-energy shoulders in photoluminescence and other hot-carrier effects.^{2,14}

For a given band and a *given number* of electron-hole pairs in their *ground states*, the maximum optical gain increases with decreasing dimensionality due to the concentration of the oscillator strength in energy. In first order, such a *k*-matched pair has the same strength, whatever the dimensionality, but occupied states usually cover a range of some $k_B T$, distributing the total oscillator strength according to the density of states. Quantized degrees of freedom allow *k* matching of the electron and hole states in the 1, 2, or 3 directions for quantum wells, wires, or boxes, respectively, and increasingly concentrate

the oscillator strength in a narrow line.

However, it should be remembered that carriers first have to cascade down to the ground state through *k-unmatched excited states*. Let us denote n, m, l as the standard (z, y, x) quantum numbers of a quantum-well, -wire, or -box system in the infinite-square-well approximation. Then, the usual $\Delta k = 0$ selection rule of optical transitions becomes $\Delta_{n,m,l} = 0$, i.e., electron and hole states can decay radiatively only if they have exactly the same three quantum numbers, n, m, l .

In typical 3D and 2D systems, electrons “meet” holes both in real and *k* space [Fig. 1(a)]. Elastic collisions very quickly randomize *k* directions (< 1 ps at laser carrier densities). Energy is lost first through LO phonon emission and next through acoustic phonons still in the subnanosecond range¹⁵ due to the 2D continuum of final states. Within their lifetime (~ 1 ns) carriers thermalize at their band edges and decay radiatively there. Going to 0D, relaxation rates vanish, chiefly due to the scarcity of final states satisfying both energy and momentum conservation. We now analyze the luminescence of a 0D box stemming from a basic quantum well of thickness L_z .

At low temperatures, LO phonon emission is severely restricted as soon as the average level spacing ΔE reaches a small fraction of the energy $\hbar\omega_{LO} \approx 30$ meV due to the near monochromaticity of LO phonons. Starting from the injecting level (a typical barrier of height 0.2–0.5 eV) a cascade with each step matching exactly $\hbar\omega_{LO}$ becomes highly unlikely. It is even more so for extreme quantization (~ 150 Å) when the spacing exceeds this energy [Fig. 1(b)].

For acoustic phonons, energy conservation selects the magnitude of the phonon wave vector $q \propto \Delta E$. However,

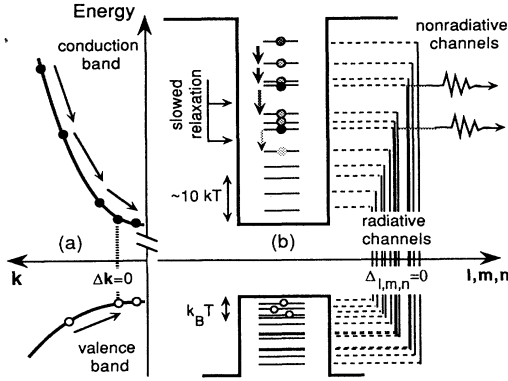


FIG. 1. (a) Energy relaxation in a continuum. Radiative recombination is possible even though $k = k'$ is needed because both band edges are populated. (b) Energy relaxation through fully-quantized box levels can be very slow. $(l, m, n) = (l', m', n')$ then is needed to decay radiatively, but this rarely occurs because nonradiative channels are efficient on electrons stored more than nanoseconds.

the momentum matrix element between the localized wave functions vanishes beyond $q \approx 2\pi/L_z$, as detailed below. Therefore, as calculated in Ref. 15, LA-phonon limited electron lifetimes increase to tens of nanoseconds below a critical confinement. Then, the cascade through the several excited l, m, n states to reach the ground state becomes longer than the usual nonradiative times (e.g., in a 2D nonetched system) [Fig. 1(b)].

As for holes, their quantization energies are less than electron ones due to their heavier mass ($m_h \approx 10m_e$). This favors thermalization of holes within some $k_B T$, as is assumed for the rest of this paper. Then, corresponding (i.e., k -matched n, m, l) electron states are in a range of $(m_h/m_e)k_B T \sim 10k_B T$ above the ground state where radiative decay is allowed.

Finally, as soon as the slowed LA-phonon relaxation sets in, electrons stay in upper box states, all of them *orthogonal* to thermalized hole states leading to strongly diminished luminescence. From Ref. 15, this occurs at $\approx 1500 \text{ \AA}$, a typical value for the observed range of the onset of the decrease of photoluminescence yield.¹⁻⁴

Turning to *intermediate temperature*, where scarcity of thermal LO phonons still holds, the $10k_B T$ range of allowed radiative decay approaches the electron-capture re-

gion (say, midbarriers). Slowed relaxation then spreads the electrons over this $10k_B T$ range ($\sim 10\text{--}100 \text{ meV}$), leading to efficient but broadened photoluminescence and laser gain curves.

At *high temperatures* energy loss occurs, rather, by a succession of two-LO or high-energy TA or LA phonons, one upward and one downward, both in the picosecond range. At very small box size and average level spacing ΔE larger than about $\hbar\omega_{LO}/2$, the two-phonon process is highly unlikely since there are no states connected by the LO-phonon energy. At larger L_x , this process becomes more likely and allows efficient relaxation. Then, as long as a few laterally confined levels lie within $k_B T$, one gets increased density of states and spectral oscillator strength compared to a 2D situation.

The most direct and cleanest way to prepare a 0D system is to place a 2D quantum well in a perpendicular quantizing magnetic field.¹⁶⁻¹⁸ The results of Berendshot, Reinen, and Bluysen on quantum-well lasers fully support the above analysis:¹⁷ at low temperatures with increasing magnetic field (i.e., smaller boxes), the threshold current increases monotonically, reflecting the hindered relaxation to the ground state. But at $\sim 120 \text{ K}$, the threshold current shows a small decrease around $B \approx 10 \text{ T}$, as we expected: at lower fields, relaxation is efficient by the two-phonon mechanism, but the number of states within $k_B T$ is hardly diminished as compared to a 2D system. At higher fields, the quantization (cyclotron) energy becomes of the order or larger than $\hbar\omega_{LO}/2$, leading to strongly decreased relaxation and an electron bottleneck in higher states not radiatively coupled to thermalized holes. In between, around 10 T , one still retains energy relaxation while having some rarefaction of electron states within $k_B T$, hence, diminishing the number of states to be inverted to obtain optical gain.

We substantiate the above ideas through a model quantum box based on the $n=1$ subband of an $L_z = 10 \text{ nm}$ $\text{In}_{0.47}\text{Ga}_{0.53}\text{As}$ well with InP barriers as in Ref. 15, or GaAs with $\text{Al}_{0.2}\text{Ga}_{0.8}\text{As}$ barriers. We use the “lateral” (l, m) energy levels of the infinitely deep square well of size $L_x, L_y > L_z$, $E_{l,m} \propto (l^2 L_x^{-2} + m^2 L_y^{-2})$ in the x - y directions, and the deformation potential, velocity of sound c_s , etc., of LA phonons as in Ref. 15. The squared matrix element, proportional to the relaxation rate between two box levels (l, m, n) , (l', m', n') has the separable form

$$\begin{aligned} M_q^{l,m,n,l',m',n'} &= |\langle \phi_{(x,y,z)}^{l'mn} | e^{iq \cdot r} | \phi_{(x,y,z)}^{l'm'n'} \rangle|^2 = M_x^{ll'}(q_x) M_y^{mm'}(q_y) M_z^{nn'}(q_z) \\ &= |\langle \phi_x^l | e^{iq_x x} | \phi_x^{l'} \rangle \langle \phi_y^m | e^{iq_y y} | \phi_y^{m'} \rangle \langle \phi_z^n | e^{iq_z z} | \phi_z^{n'} \rangle|^2, \end{aligned} \quad (1)$$

where the ϕ 's are the usual square-well quantized envelope functions. M_x and M_y yield factors of the form $\sin[q_x L_x/2 \pm (l \pm l')/(2\pi)]$, while M_z yields for the intra-band transitions $n = n' = 1$ of interest here $\sin q_z L_z/2$.

The level spacing $\Delta E \propto [(l'^2 + m'^2) - (l^2 + m^2)]L_x^{-2} = pL_x^{-2}$ imposes the magnitude of the phonon wave vector $q = \Delta E/(\hbar c_s)$. So q scales like L_x^{-2} , whereas the typical extent π/L_x of M_x (M_y) scales like L_x^{-1} and is much smaller than the extent $\sim \pi/L_z$ of M_z which arises from the main confinement controlled by the epitaxial layer

growth. Hence, for L_x much narrower than the characteristic “phonon length” $L_1 = \hbar/2m^*c_s$, and thus $\Delta E \gg E_1 = m^*c_s^2$, energy conservation requires $q \gg \pi/L_x$. Therefore, only phonons with $q_x \sim \pi/L_x \ll q$ and $q_z \approx q$ interact. Here, $m^* \approx 0.041m_0$, so $L_1 \approx 2.6 \text{ \mu m}$ and $E_1 \approx 2.7 \text{ \mu eV}$. At this stage, however, the scattering rate still increases with confinement.¹⁵ On further confining at $\Delta E > \Delta E_0 \approx \hbar c_s(2\pi)/L_z \approx 0.6 \text{ meV}$, M_z also vanishes and relaxation is *annihilated* within a 20%–50% variation of q , i.e., a 10%–20% variation of L_x . This is because

$M_z(q) \propto q^{-6} \propto L_x^{12}$ in this region. The particular value $L_x = L_0$ where ΔE reaches ΔE_0 and M_z vanishes also depends on $p = (l'^2 + m'^2) - (l^2 + m^2)$. In this respect, the value $p=3$ [(2,1) \rightarrow (1,1)] in Ref. 15 gives $L_0 = (L_1 L_2)^{1/2} \approx 160$ nm. A close examination of realistic box situations proves it more reasonable to consider about a hundred levels ($l, m \sim 10$). Then the value of p between neighbor levels spans the range 1–8. For higher p values, the slowed relaxation happens at even larger L_x values. Hence, our simulation takes into account the fact that in actual boxes, neighbor level spacings are distributed and it includes the uppermost spacing values in the cascade as they act as bottlenecks first. Two refinements were introduced: (i) The exact square box has no spacing smaller than $p=1$ and all levels are twice degenerate, which seems unrealistic. Examining a variety of cases, we found that a 5% size difference between the two sides yields a representative and realistic distribution of level spacing while still relevant to the perfect square box. (ii) Due to this modification, levels can be accidentally very close and thus strongly coupled and equilibrated at any time. Then we group them as a single degenerate level. With these criteria, we end up with 85 electron states in 66 levels. We then compute the transition rates due to LA-phonon scattering between all pairs of levels assuming $L < L_1$. In this regime, the above consideration on the extent of M_x and M_z leads to the following approximation:

$$w_{ij} = CL_x^{-4} [n_B(q) + \{\delta\}] M_z(q), \quad (2)$$

where $n_B(q)$ is the phonon occupancy number and C is a constant. In the curly brackets, 1 stands for phonon emission and 0 for phonon absorption. Let us stress that the regime of vanishing relaxation implies $M_z(q) \propto L_x^{12}$ and thus $w_{ij} \propto L_x^8$, a very fast decrease with lateral confinement. It is assumed that holes are thermalized with their Fermi energy at ground level so that the radiative decay rates of electrons at energy E above the ground state can be written as $w_{\text{rad}}(E) = (\tau_r)^{-1} (\exp[(m_h/m_e) \times E/k_B T] + 1)^{-1}$ with $m_h/m_e = 10$ and $\tau_r = 1.6$ ns. The nonradiative decay rate is taken constant and equal to $w_{\text{NR}} = \tau_{\text{NR}}^{-1} = 0.1$ ns $^{-1}$. Capture is taken into account by imposing an occupancy $\frac{1}{2}$ to the upper level E_{max} at any time. In the absence of any recombination, this would be the Fermi energy. We then iterate a Pauli master equation on the occupation probabilities p_i of the levels:

$$\frac{dp_i}{dt} = -w_{ii}p_i + \sum_{j \neq i} [w_{ji}p_j(1-p_i) - w_{ij}p_i(1-p_j)], \quad (3)$$

where $w_{ii} = w_{\text{rad}}(E_i) + w_{\text{NR}}$. After a few τ_{NR} , a stationary state is reached and fluxes are computed for the radiative and nonradiative decay channels. Figure 2 shows such stationary solutions at 4 K in the slow relaxation regime: carriers clearly accumulate whenever a larger ΔE induces a slow relaxation and reach a dynamic equilibrium by feeding the nonradiative channel if they are above $\sim 10k_B T$ of the ground state. Figure 3 shows the radiative yield, i.e., the fraction of electrons decaying radiatively, for the $\text{In}_{0.47}\text{Ga}_{0.53}\text{As}$ and the GaAs well cases, which basically differ in effective mass. The expected decrease of the radiative efficiency shows up around $L_x = 200$ nm and is very fast below. We claim that the effect is quite

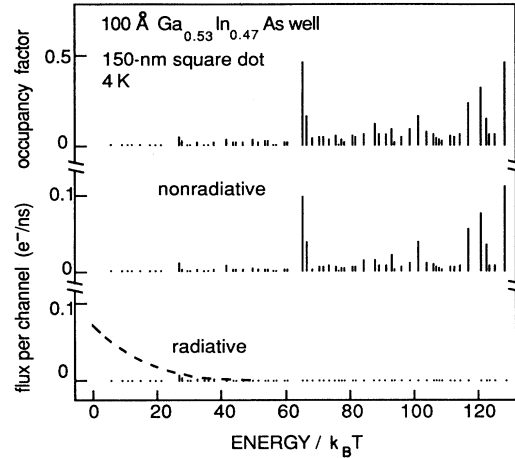


FIG. 2. Occupancy (upper part), nonradiative flux (middle part), and radiative flux (bottom part) of the 66 levels of a quantum box at 4 K of size $L_x = 150$ nm for the 100-Å $\text{Ga}_{0.53}\text{In}_{0.47}\text{As}/\text{InP}$ well system as a function of the reduced energy ($E/k_B T$). The dashed line schematizes the radiative probability reflecting the thermal hole distribution.

independent of any adjustable parameter as large variations of the nonradiative rate in either direction by 1 or 2 orders of magnitude would only slightly shift the shoulder due to the very sudden occurrence of slowed relaxation with decreased size.

To go toward quantum wires, we take $L_x = aL_y$ with $a = 10$. Looking at the largest level spacings, we now predict the cascade through the (high $l, m=1$) levels just below $l=1, m=2$ to be the bottleneck. Simple calculations show that ΔE scales like a in this region, reaching ΔE_0 at $L_y = L_0 a^{-1/2}$. This is pictured in Fig. 3, where the onset of decay is at ~ 70 nm instead of ~ 200 nm for quantum boxes. Plausibly, this can be applied to a true (infinite) wire if we say that electron diffusion events or accidental constrictions of the wire due to nearby impurities occur about every $L_x = aL_y$, 500–1000 nm in this case.

However, another recombination mechanism sets in, due to carrier transport: even though defect density is not largely increased when compared to 2D or 3D (we claim here that we need not a major defect on each quantum

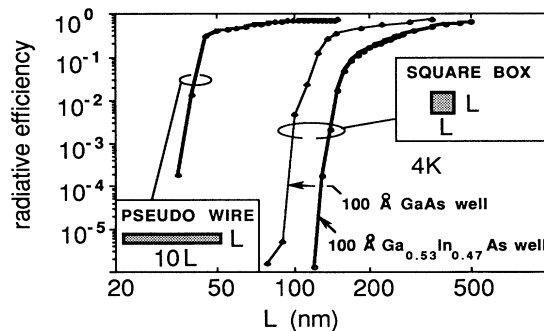


FIG. 3. Log-log plot of the radiative efficiency of square ($L \times L$) quantum boxes and ($L \times 10L$) pseudo wires on 100-Å well in the $\text{In}_{0.47}\text{Ga}_{0.53}\text{As}/\text{InP}$ and the GaAs/ $\text{Al}_{0.2}\text{Ga}_{0.8}\text{As}$ system as a function of the lateral dimension L at 4 K.

box to explain their poor efficiency), one can still find a major defect within a diffusion length of an electron in a quantum wire, and this defect can be reached within the carrier lifetime. This effect has been recently seen in the careful study of photoluminescence efficiency on quantum wires of different lengths.¹⁹ The quantum efficiency increases with decreasing wire length for thin wires ($< 3 \mu\text{m}$), evidencing the statistical appearance of defect-free wires at small lengths, with an increased quantum efficiency.

In conclusion, we claim that the poor efficiency of quantum boxes in photoluminescence and laser action is due to the combination of inefficient energy relaxation and ortho-

gonality of carrier quantum states, rather than to a major increase in extrinsic defect density. Model calculations of acoustic-phonon relaxation support this effect. The mechanisms are also well evidenced in the quantum-well-laser studies in magnetic fields as a function of temperature.

One of us (C.M.S.-T.) would like to thank the Nuffield Foundation for financial support. This work has been supported in part under the ESPRIT Basic Research Action No. 3133. Fruitful discussions with U. Bockelmann, J. Favre, B. Vinter, and Y. Perréal are gratefully acknowledged.

-
- ¹M. Kohl, D. Heitmann, W. W. Rühle, P. Grambow, and K. Ploog, *Phys. Rev. B* **41**, 12 338 (1990).
- ²J. N. Patillon, C. Jay, M. Iost, R. Gamonal, J. P. André, B. Soucaïl, C. Delalande, and M. Voos, *Superlattices Microstruct.* **8**, 335 (1990).
- ³M. Notomi, M. Naganuma, T. Nishida, T. Tamamura, H. Iwamura, S. Nojima, and M. Okamoto, *Appl. Phys. Lett.* **58**, 720 (1991).
- ⁴H. Leier, A. Forchel, B. E. Maile, G. Mayer, J. Hommel, G. Weimann, and W. Schlapp, *Appl. Phys. Lett.* **56**, 48 (1989).
- ⁵H. E. G. Arnot, M. Watt, C. M. Sotomayor-Torrès, R. Glew, R. Cuso, J. Bates, and S. P. Beaumont, *Superlattices Microstruct.* **5**, 459 (1989).
- ⁶H. E. G. Arnot, C. M. Sotomayor-Torrès, R. Cusco, M. Watt, R. Glew, and S. P. Beaumont, *Quantum Wells for Optics and Optoelectronics*, Technical Digest Series Vol. 10. (Optical Society of America, Washington, DC, 1989), p. 83; C. M. Sotomayor-Torrès, M. Watt, H. E. G. Arnot, R. Glew, R. Cusco Cornet, T. M. Kerr, S. Thoms, and S. P. Beaumont, *Surf. Sci.* **228**, 275 (1990).
- ⁷D. Lootens *et al.* (unpublished).
- ⁸M. Cao, P. Daste, Y. Miyamoto, Y. Miyake, S. Nigowa, S. Arai, K. Furuya, and Y. Suematsu, *Electron. Lett.* **24**, 824 (1988).
- ⁹E. Kapon, S. Simhony, R. Bhat, and D. M. Hwang, *Appl. Phys. Lett.* **55**, 2715 (1989).
- ¹⁰Y. Arakawa and H. Sakaki, *Appl. Phys. Lett.* **40**, 939 (1982).
- ¹¹Y. Arakawa, H. Sakaki, M. Nishioka, H. Okamoto, and N. Miura, *Jpn. J. Appl. Phys.* **22**, 804 (1983).
- ¹²Y. Miyamoto, M. Asada, and Y. Suematsu, *IEEE J. Quantum Electron.* **QE-25**, 2001 (1989).
- ¹³M. A. Reed, R. T. Bate, K. Bradshaw, W. M. Duncan, W. R. Frensley, J. W. Lee, and H. D. Shih, *J. Vac. Sci. Technol. B* **4**, 358 (1986).
- ¹⁴G. Mayer, H. Leier, B. E. Maile, A. Forchel, H. Schweizer, G. Weimann, and W. Schlapp, in *Proceedings of the 20th International Conference on the Physics of Semiconductors*, edited by E. M. Anastassakis and J. D. Joannopoulos (World Scientific, Singapore, 1990), p. 2415.
- ¹⁵U. Bockelmann and G. Bastard, *Phys. Rev. B* **42**, 8947 (1990).
- ¹⁶J. C. Maan, M. Potemski, K. Ploog, and G. Weimann, edited by F. Kuchar, H. Heinrich, and G. Bauer, *Springer Series in Solid-State Sciences Vol. 97* (Springer-Verlag, Berlin, 1990), p. 285.
- ¹⁷T. T. J. M. Berendschot, H. A. J. M. Reinen, and H. J. A. Bluyssen, *Appl. Phys. Lett.* **54**, 1827 (1989).
- ¹⁸Y. Arakawa, H. Sakaki, M. Nishioka, H. Okamoto, and N. Miura, *Jpn. J. Appl. Phys.* **22**, L804 (1983).
- ¹⁹W. E. Leitch (unpublished).